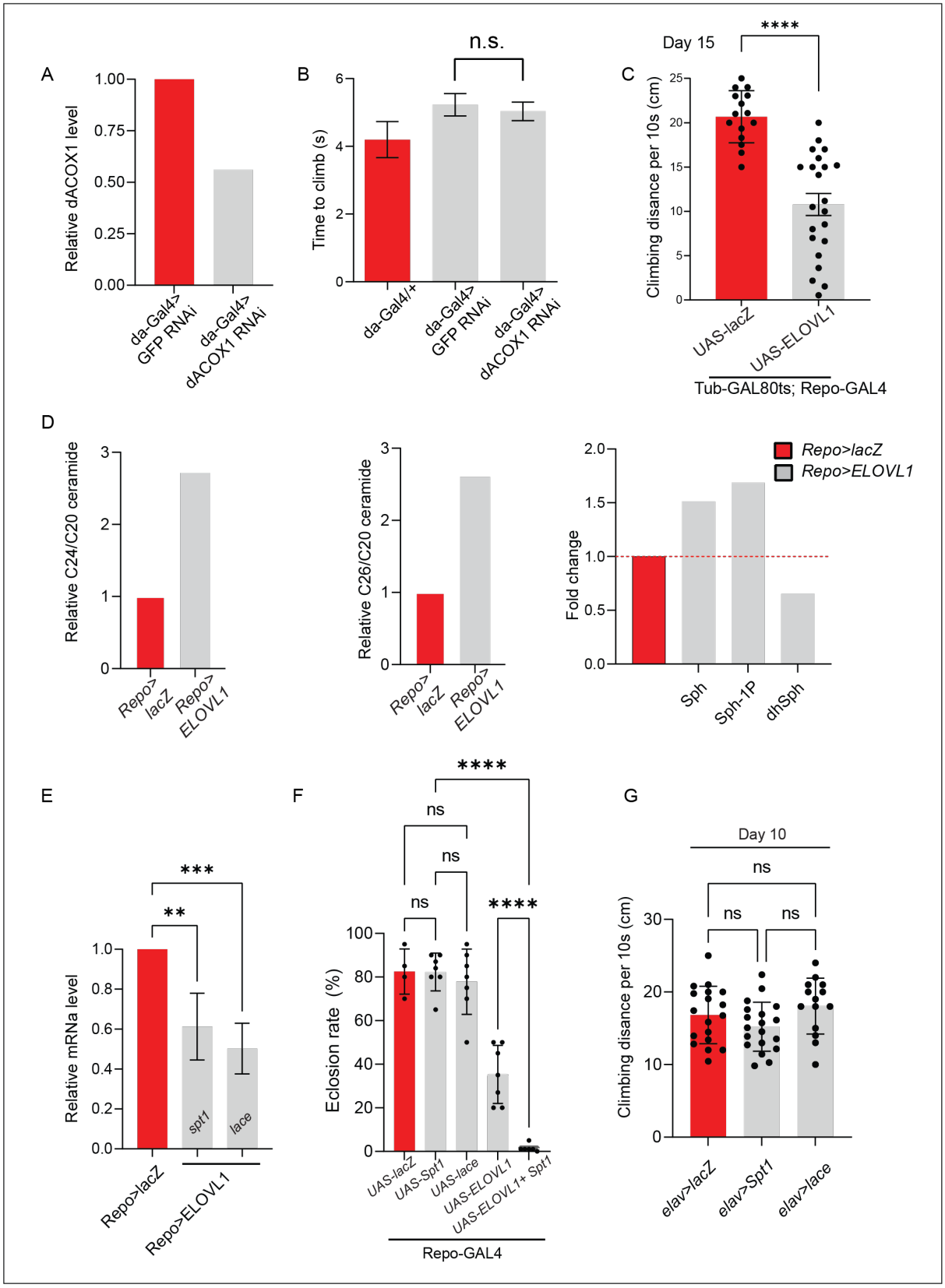
A
Relative dACOX1 level
1.00
0.75
0.50
0.25
0.00
da-Gal4> GFP RNAi
da-Gal4> dACOX1 RNAi
B
n.s.
Time to climb (s)
6
4
2
0
da-Gal4/+
da-Gal4> GFP RNAi
da-Gal4> dACOX1 RNAi
C
Day 15
****
Climbing disance per 10s (cm)
25
20
15
10
5
0
UAS-lacZ
UAS-ELOVL1
Tub-GAL80ts; Repo-GAL4
D
Relative C24/C20 ceramide
3
2
1
0
Repo> lacZ
Repo> ELOVL1
Relative C26/C20 ceramide
3
2
1
0
Repo> lacZ
Repo> ELOVL1
Repo>lacZ
Repo>ELOVL1
Fold change
2.0
1.5
1.0
0.5
0.0
Sph
Sph-1P
dhSph
E
***
**
Relative mRNA level
1.0
0.8
0.6
0.4
0.2
0.0
spt1
lace
Repo>lacZ
Repo>ELOVL1
F
****
ns
ns
ns
****
Eclosion rate (%)
100
80
60
40
20
0
UAS-lacZ
UAS-Spt1
UAS-lace
UAS-ELOVL1
UAS-ELOVL1+ Spt1
Repo-GAL4
G
Day 10
ns
ns
ns
Climbing disance per 10s (cm)
30
20
10
0
elav>lacZ
elav>Spt1
elav>lace

Figure S1. Glial ELOVL1 expression causes neurodegenerative phenotypes and increases the levels of VL-Ceramides and S1P (Related to Figure 1).

(A) *dACOX1 RNAi* only reduces the ACOX1 protein levels by less than 50%. (B) Ubiquitous expression of *dACOX1 RNAi* failed to induce climbing defects on Day 20. (n>20 per genotype). (C) Climbing assays on Day 15 for the flies (*Tub-GAL80ts; Repo-GAL4>ELOVL1*). Flies were raised at 18°C (no expression of *ELOVL1*) and shifted to 29°C 1-3 days after eclosion (high expression of *ELOVL1*). (D) Expression of *ELOVL1* in glia results in a 3-fold elevation of VL-Ceramide and a 1.6 fold elevation of Sphingosine phosphates compared to control (*Repo>lacZ*). Note that whole adult heads were used for lipidomic analysis, and glia correspond to less than 10% of the whole-brain population in fly CNS. (E) The transcript level of SPT enzymes (Lace and Spt1) in control (*Repo>lacZ*) and *Repo>ELOVL1* flies. (F) Eclosion rates of flies that express *UAS-lacZ* (control), *UAS-Spt1*, *UAS-lace*, *UAS-ELOVL1*, or *UAS-ELOVL1+Spt1* in glia. Quantification of the percentage of expected animals per cross (n>4). (G) Climbing assays on Day 10 (*elav>lacZ*, *elav>Spt1*, and *elav>lace*). Eclosion rates were not significantly affected in these flies (n>15 per genotype). Statistical analyses are one-way ANOVA followed by a Tukey post hoc test. Results are mean ± s.e.m. (****$p < 0.0001$, ***$p < 0.001$, **$p < 0.01$; n.s., not significant).

Figure S2

A

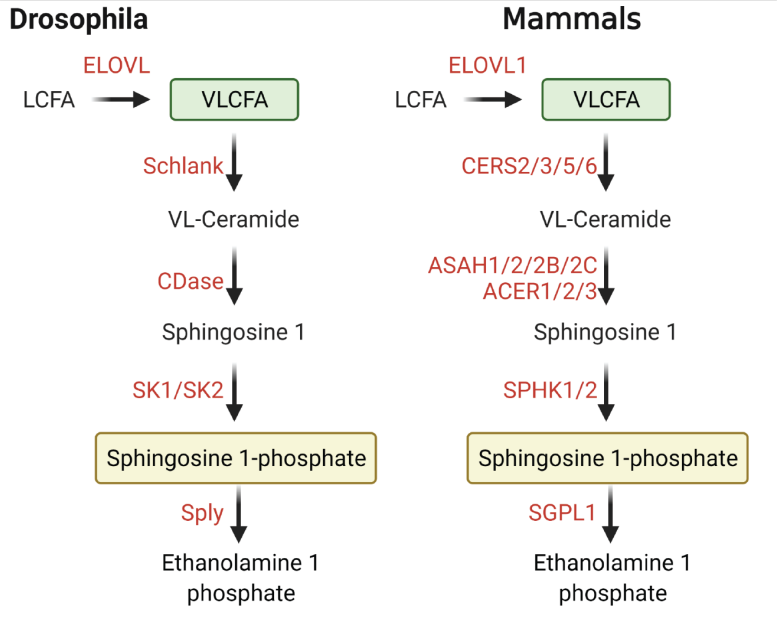

B. Generation of *CDase*^{T2A}

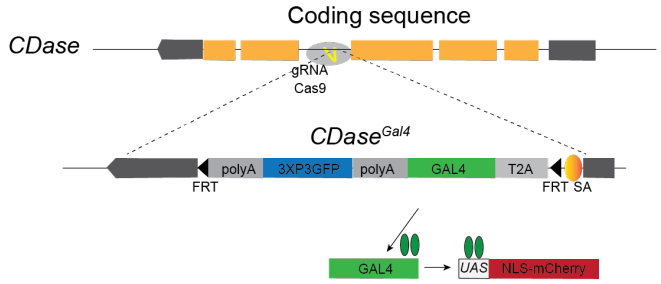

C. Generation of *SK1*^{KG4}

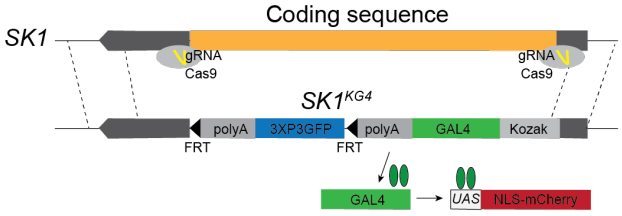

D. Generation of *CDase*^{null}

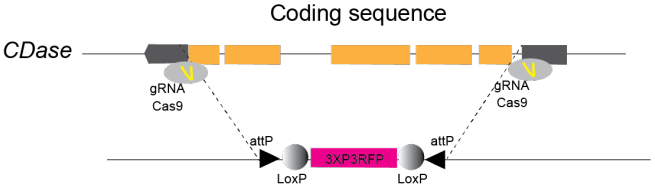

Figure S2. Strategies to create the *CDase^{T2A}*, *SK1^{T2A}*, and *CDase^{null}* alleles (Related to Figure 2).

(A) Comparison of the key players implicated in the S1P exit pathway in flies and mammals. Note that mammals have many paralogous enzymes in the S1P exit pathway, whereas the fly S1P exit pathway has few. (B) CRIMIC constructs for *CDase^{T2A},* (C) and *SK1^{T2A},* (D) Generation of the *CDase^{null}* allele.

Figure S3

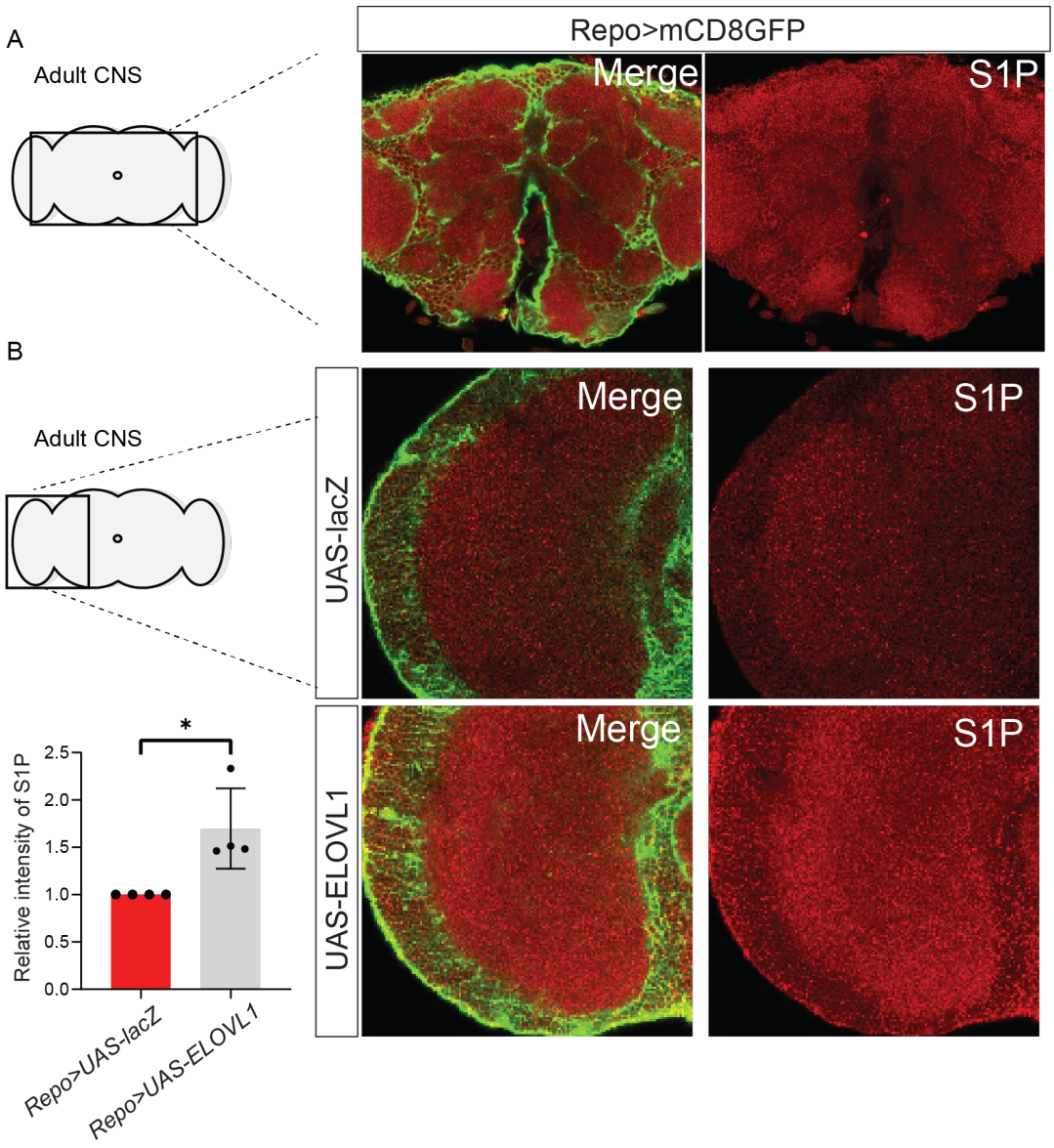
A
Adult CNS
Repo>mCD8GFP
Merge
S1P
B
Adult CNS
UAS-lacZ
UAS-ELOVL1
Merge
S1P
Merge
S1P
*
Relative intensity of S1P
2.5
2.0
1.5
1.0
0.5
0.0
Repo>UAS-lacZ
Repo>UAS-ELOVL1

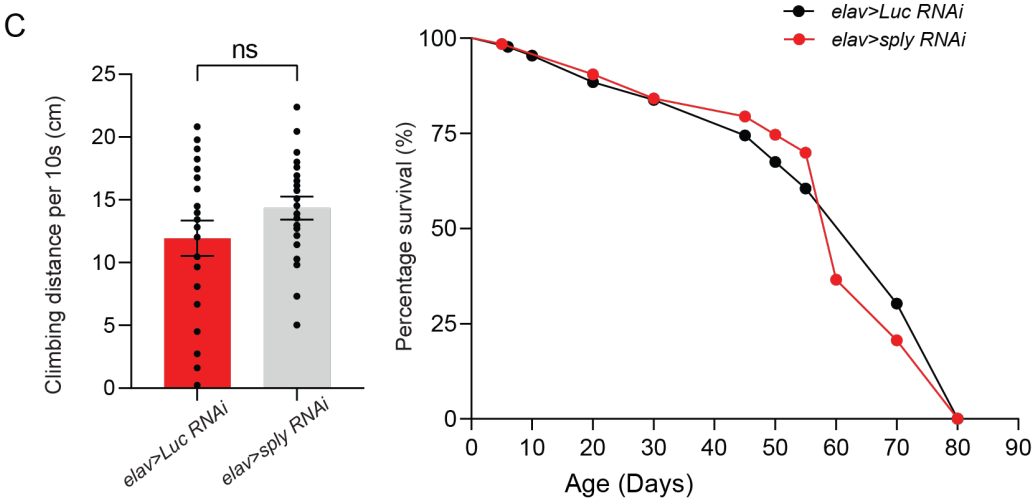
C
ns
Climbing distance per 10s (cm)
25
20
15
10
5
0
elav>Luc RNAi
elav>sply RNAi
elav>Luc RNAi
elav>sply RNAi
Percentage survival (%)
100
75
50
25
0
0
10
20
30
40
50
60
70
80
90
Age (Days)

Figure S3. S1P accumulates in the adult CNS (Related to Figure 3).

(A) Adult brain. Green marks the glial membrane (Repo>mCD8GFP), and Red indicates S1P. (B) Optic lobes. Top: *Repo>mCD8GFP*, Bottom: *Repo>ELOVL1*. The images were taken as stacks, and a similar section was analyzed for the quantifications (left), n=4 per genotype. (C) Behavioral phenotypes of flies in which the levels of *sply* in neurons is decreased (*elav>sply RNAi*). Left: climbing assays, Right: life-span. n>20. Results are mean ± s.e.m. (n.s., not significant). Statistical analyses are one-way ANOVA followed by a Tukey post hoc test. Results are mean ± s.e.m. (*$p < 0.01$; n.s., not significant).

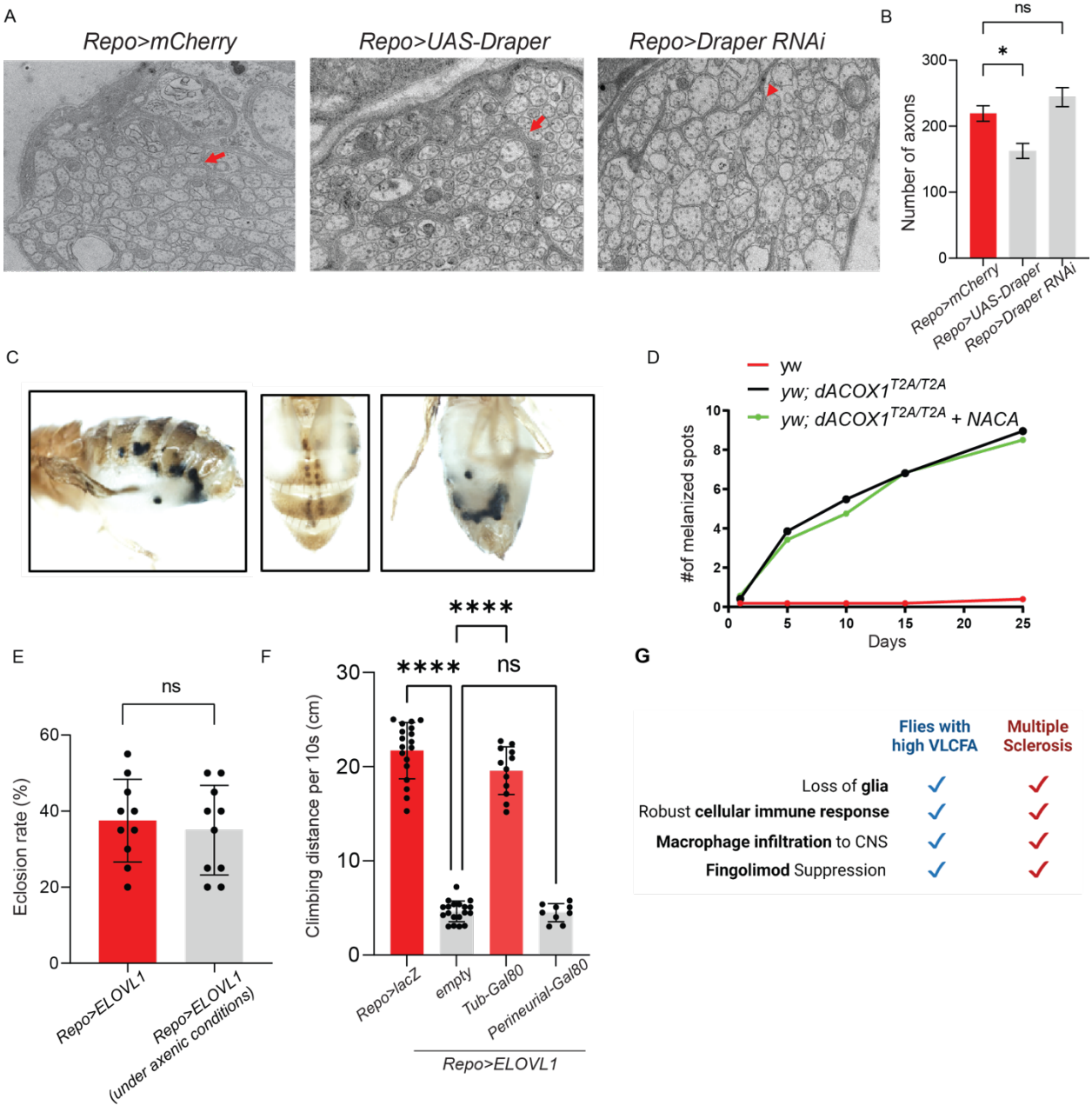
A
Repo>mCherry
Repo>UAS-Draper
Repo>Draper RNAi
B
ns
*
Number of axons
300
200
100
0
Repo>mCherry
Repo>UAS-Draper
Repo>Draper RNAi
C
D
yw
yw; dACOX1T2A/T2A
yw; dACOX1T2A/T2A + NACA
#of melanized spots
Days
E
ns
Eclosion rate (%)
Repo>ELOVL1
Repo>ELOVL1 (under axenic conditions)
F
****
ns
Climbing distance per 10s (cm)
Repo>lacZ
empty
Tub-Gal80
Perineurial-Gal80
Repo>ELOVL1
G
Flies with high VLCFA
Multiple Sclerosis
Loss of glia
Robust cellular immune response
Macrophage infiltration to CNS
Fingolimod Suppression

Figure S4. Progressive melanization phenotypes (Related to Figure 6).

(A) Image of a section of the wing nerve. Glial Draper expression (*Repo>UAS-Draper*) leads to extended and expanded glial membranes compared to control (*Repo>mCherry*); however, Draper RNAi (Repo>Draper RNAi) reduces the size of glial membrane (see red arrows). (B) The number of axons is significantly reduced in the wing margin nerves of *Repo>Draper* flies but not in *Repo>Draper RNAi* flies at Day 3 (n=3 per each genotype). (C) $dACOX1^{T2A}$ mutants, exhibit robust melanization phenotypes in abdomen, nephrocytes, and fat bodies. (D) Supplementation of NACA (AD4) fails to suppress the melanization phenotypes. (E) Eclosion rate of the Repo>ELOVL1 flies raised and kept in axenic conditions following the protocol described in Koyle et al., (2016) compared to Repo>ELOVL1 flies under normal conditions at 25°C. n=10 per genotype. (F) Climbing assays on Day 10 for the flies expressing ubiquitous or perineurial *Gal80* in the background of *Repo>ELOVL1* (genotypes are described in the graph). (G) Summary and comparison of phenotypes of flies with elevated levels of VLCFA in glia (blue) and MS patients (red). Statistical analyses are one-way ANOVA followed by a Tukey post hoc test. Results are mean ± s.e.m. (****$p < 0.0001$, ***$p < 0.001$, **$p < 0.01$; n.s., not significant).

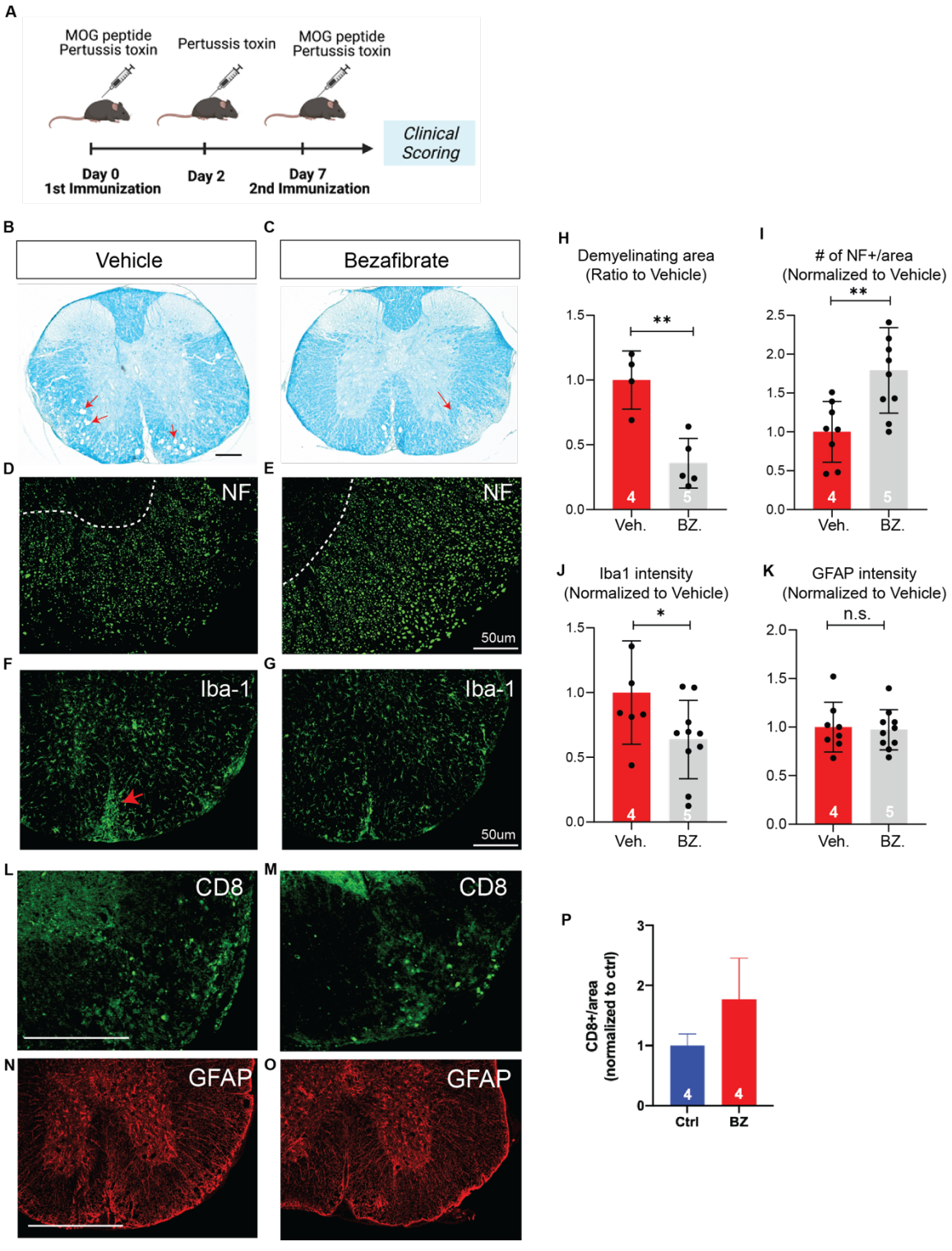
A
MOG peptide
Pertussis toxin
Pertussis toxin
MOG peptide
Pertussis toxin
Clinical Scoring
Day 0
1st Immunization
Day 2
Day 7
2nd Immunization
B
Vehicle
C
Bezafibrate
D
NF
E
NF
50um
F
Iba-1
G
Iba-1
50um
L
CD8
M
CD8
N
GFAP
O
GFAP
H
Demyelinating area
(Ratio to Vehicle)
**
1.5
1.0
0.5
0.0
4
5
Veh.
BZ.
I
# of NF+/area
(Normalized to Vehicle)
**
2.5
2.0
1.5
1.0
0.5
0.0
4
5
Veh.
BZ.
J
Iba1 intensity
(Normalized to Vehicle)
*
1.5
1.0
0.5
0.0
4
5
Veh.
BZ.
K
GFAP intensity
(Normalized to Vehicle)
n.s.
2.0
1.5
1.0
0.5
0.0
4
5
Veh.
BZ.
P
CD8+/area
(normalized to ctrl)
3
2
1
0
4
4
Ctrl
BZ

Figure S5. **Prophylactic bezafibrate treatment does not alter the number of CD8+ T cells and reactive astrocytes in EAE mice (Related to Figure 7).**

(A) An overall scheme of EAE induction in mice (B-C) Spinal cord sections from the EAE mice were stained by Luxol fast blue (LFB) to assess the demyelination (n = 4-5 per group). (D-G) Immunostaining of neurofilament (NF) and Iba-1 for neuronal loss and microglia/macrophage infiltration analysis (n = 4-5 per group). (H-K) Quantifications of LFB, NF, IBA1, and GFAP staining. Each data point represents individual images from multiple animals. (L-O) Spinal cord sections from the EAE mice were stained by CD8 and GFAP to assess T cell infiltration and reactive astrocytes (n =4 per group). (P) Quantifications of CD8 positive cells per area. Values were normalized to vehicle-treated control and statistically analyzed by unpaired Student's t-test. Data in all figures are represented as mean ± SEM * $p < 0.05$, ** $p < 0.01$.

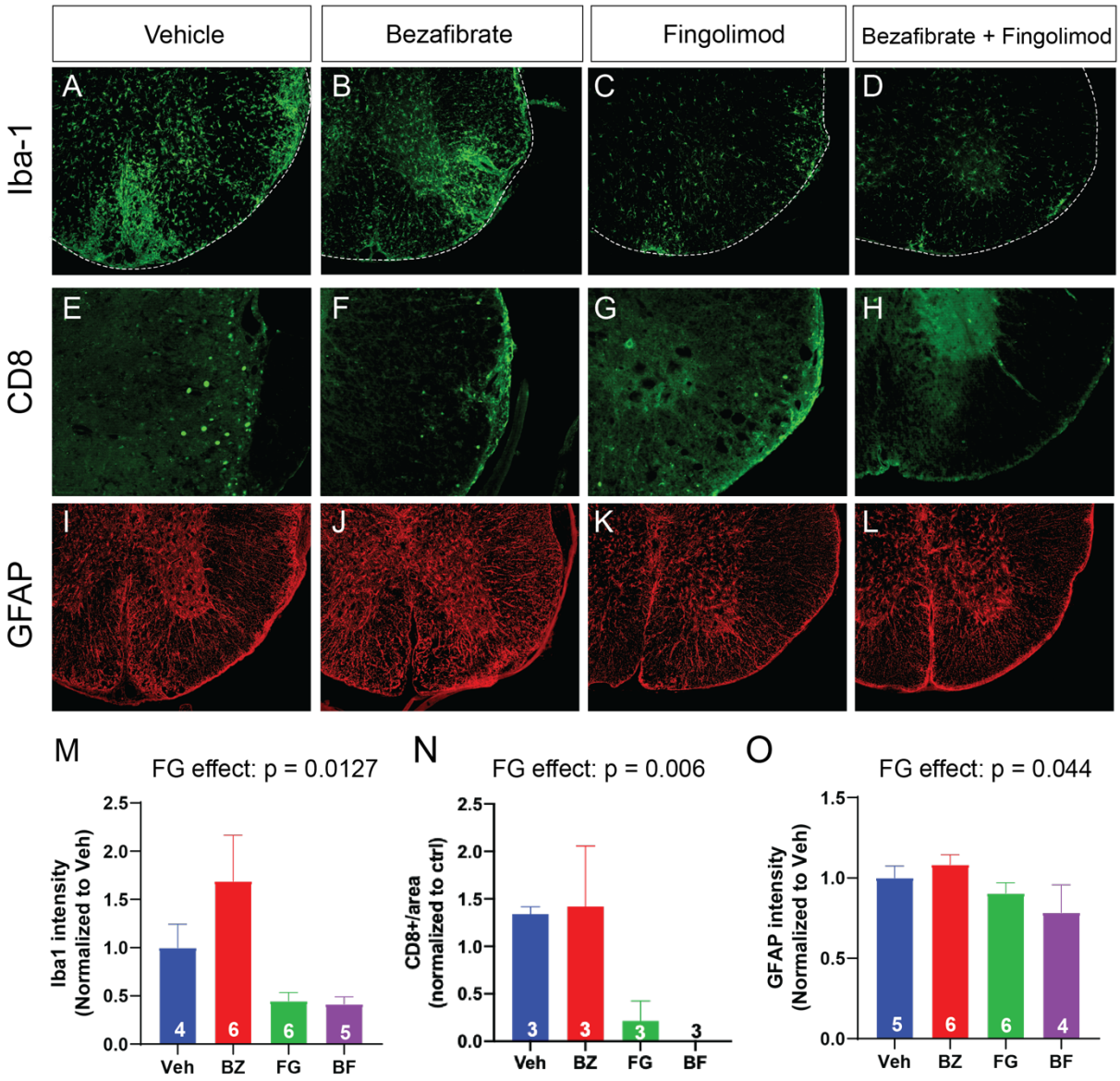
Vehicle
Bezafibrate
Fingolimod
Bezafibrate + Fingolimod
Iba-1
CD8
GFAP
A
B
C
D
E
F
G
H
I
J
K
L
M
FG effect: p = 0.0127
Iba1 intensity (Normalized to Veh)
2.5
2.0
1.5
1.0
0.5
0.0
4
6
6
5
Veh
BZ
FG
BF
N
FG effect: p = 0.006
CD8+/area (normalized to ctrl)
3
3
3
3
O
FG effect: p = 0.044
GFAP intensity (Normalized to Veh)
1.5
1.0
0.5
0.0
5
6
6
4

Figure S6. Fingolimod, but not Bezafibrate, suppresses immune cell infiltration and reactive astrocyte activation in EAE mice (Related to Figure 7).

(A-L) Spinal cord sections from the EAE mice were stained by Iba1 (microglia/macrophage), CD8 (T cells), and GFAP (reactive astrocytes) (n =3-6 per group). (M-O) Quantifications of CD8. (P) The number of CD4+ T cells is low at chronic stage of EAE, whereas some CD8+ T cells remain. Values were normalized to vehicle-treated control and statistically analyzed using two-way ANOVA, followed by Sidak post-hoc analysis, * $p < 0.05$, ** $p < 0.01$. Data in all figures are represented as mean ± SEM.